



Ultrastrong, Stiff and Multifunctional Carbon Nanotube Composites

X. Wang, Z.Z. Yong, Q.W. Li, P.D. Bradford, W. Liu, D.S. Tucker, W. Cai, H. Wang, F.G. Yuan & Y.T. Zhu

To cite this article: X. Wang, Z.Z. Yong, Q.W. Li, P.D. Bradford, W. Liu, D.S. Tucker, W. Cai, H. Wang, F.G. Yuan & Y.T. Zhu (2013) Ultrastrong, Stiff and Multifunctional Carbon Nanotube Composites, *Materials Research Letters*, 1:1, 19-25, DOI: [10.1080/21663831.2012.686586](https://doi.org/10.1080/21663831.2012.686586)

To link to this article: <https://doi.org/10.1080/21663831.2012.686586>



Copyright X. Wang, Z. Z. Yong, Q. W. Li, P. D. Bradford, W. Liu, D. S. Tucker, W. Cai, H. Wang, F. G. Yuan and Y. T. Zhu



[View supplementary material](#)



Published online: 11 Oct 2012.



[Submit your article to this journal](#)



Article views: 10197



[View related articles](#)



Citing articles: 25 [View citing articles](#)

Ultrastrong, Stiff and Multifunctional Carbon Nanotube Composites

X. Wang^a, Z. Z. Yong^b, Q. W. Li^{b,*}, P. D. Bradford^a, W. Liu^a, D. S. Tucker^c, W. Cai^d, H. Wang^d,
F. G. Yuan^e and Y. T. Zhu^{a,*}

^aDepartment of Materials Science and Engineering, North Carolina State University, Raleigh, NC 27695, USA

^bSuzhou Institute of Nano-Tech and Nano-Bionics, Suzhou 215125, China

^cMaterials and Processes Laboratory, Marshall Space Flight Center, AL 35812, USA

^dHigh Temperature Materials Laboratory, Oak Ridge National Laboratory, Oak Ridge, TN 37831, USA

^eDepartment of Mechanical and Aerospace Engineering, North Carolina State University, Raleigh, NC 27695, USA

(Received 18 February 2012; final form 22 March 2012)

Supplementary Material Available Online

Carbon nanotubes (CNTs) are an order of magnitude stronger than any other current engineering fiber. However, for the past two decades, it has been a challenge to utilize their reinforcement potential in composites. Here, we report CNT composites with unprecedented multifunctionalities, including record high strength (3.8 GPa), high Young's modulus (293 GPa), electrical conductivity ($1230 \text{ S} \cdot \text{cm}^{-1}$), and thermal conductivity ($41 \text{ W m}^{-1} \text{ K}^{-1}$). These superior properties are derived from the long length, high volume fraction, good alignment and reduced waviness of the CNTs, which were produced by a novel-processing approach that can be easily scaled up for industrial production.

Keywords: Carbon Nanotubes, Composite Materials, Tensile Strength, Multifunctional, Alignment

Since their discovery [1], carbon nanotubes (CNTs) have been predicted to have the potential to make the next-generation composite structures with unprecedented strength and stiffness to meet the demands of future space explorations. In addition, their high thermal and electrical conductivities [2] render CNTs potential to impart multifunctionalities to the composites for applications such as electromagnetic wave absorption, *in situ* monitoring of structures, lightning-strike prevention, and heat dissipation. The challenge is how to obtain well-dispersed and high volume fractions of long and straight CNTs in the composite for high performance, and how to develop a scalable technology for industrial production.

CNT composites fabricated by conventional methods [3–6] have not exhibited the exceptional mechanical properties promised by their nanoscale building blocks. For the most widely used dispersion method, the constituent nanotubes underperform when fabricated into composites, which is mainly due to CNT agglomeration and low volume fractions (usually <5%). Buckypaper or CNT arrays can be utilized to fabricate composites

at fast processing rates. Newly developed approaches such as ‘domino-pushing’ [7] or ‘shear-pressing’ [8] can produce controllable structures of CNTs and good CNT alignment. Mechanical alignment, functionalization and subsequent infiltration of CNT buckypaper with bismaleimide (BMI) matrix produced composites with a high strength of about 3 GPa, which are the strongest CNT nanocomposites reported to date [9]. However, the waviness of individual CNTs has limited the further improvement of the composite strength.

Since the report of a dry-drawing method in 2002 [10], much effort has been focused on scaling up the growth of superaligned CNT arrays [11–13]. Due to their high-purity, high-quality and ordered structure, the superaligned CNT arrays can be converted into continuous fibers or sheets in the dry state [2,10,11,14–18]. These fibers and sheets, within which the nanotubes possess a high degree of alignment, have also been incorporated into polymer matrices to make strong CNT/polymer composite fibers [19–21]. For example, CNT/PVA (polyvinyl alcohol) composite fibers have

*Corresponding author. ytzhu@ncsu.edu or qwli2007@sinano.ac.

been reported to have a high tensile strength of 2.0 GPa, a Young's modulus over 120 GPa, and an electrical conductivity of $920 \text{ S} \cdot \text{cm}^{-1}$ [19]. However, low production rate limits their application as reinforcement of macroscopic composites. By dry-drawing and stacking CNT sheets and then infiltrating the stack with epoxy resin, Cheng *et al.* [22,23] produced composites with desired structural characteristics. However, the fluffy CNT network and wavy individual nanotubes resulted in composites with relatively low mechanical properties. Recently, a spray winding approach was developed to wind onto a rotating spool CNT sheet from superaligned CNT array and simultaneously apply polymer solution onto each layer of CNTs [24,25]. This approach has created CNT composite sheets with a toughness, strength and electrical conductivity up to 100 J/g , 1.8 GPa and $780 \text{ S} \cdot \text{cm}^{-1}$, respectively [24]. The spray winding approach is advantageous in terms of the capability to preserve CNT alignment, easy fabrication and potential for industrial scale-up.

One critical issue that prevents the full utilization of strengthening potential of CNTs is their waviness. Wavy CNTs do not carry the load at the same time, cannot be packed densely, and have poor inter-tube contacts, all of which adversely affect the strength, stiffness, and conductivity of resulting CNT composites.

In this work, we report a novel stretch-winding process for fabricating high volume-fraction ($\sim 46\%$) CNT/polymer composites with a combined strength and Young's modulus that is not accessible to any current carbon fiber-reinforced polymer (CFRP) composites. When the CNT sheet was stretched by 12%, a tensile strength of up to 3.8 GPa and Young's modulus of up to 293 GPa were achieved for the composite. It also showed a high thermal conductivity of $41 \text{ W m}^{-1} \text{ K}^{-1}$ and electrical conductivity of $1230 \text{ S} \cdot \text{cm}^{-1}$.

Fabrication of CNT Composite Sheets by Stretch-winding Process The key component of our strategy for fabricating high-strength CNT composites is to straighten the wavy CNTs before embedding them into a polymer matrix, as illustrated in Figure 1(a). The unidirectional CNT sheets used in this study were converted from superaligned CNT arrays that were synthesized by a chemical vapor deposition method [11]. The CNTs were multi-walled (MWNTs) with outer diameter of 7–9 nm and 4–6 walls (as shown in the Supplementary online material). The density of the nanotube was calculated as $1.51 \text{ g} \cdot \text{cm}^{-3}$ based on the average CNT inner and outer diameters. The strong van der Waals inter-tube interaction enables the drawing of continuous and uniform CNT sheets, in which the CNTs are largely aligned in the drawing direction. However, individual nanotubes are wavy microscopically, as demonstrated in a previous work [26].

In a stretch-winding process as shown in Figure 1(b), the CNT sheet travels horizontally and passes through a tensioning system. As the CNT sheet passes around a

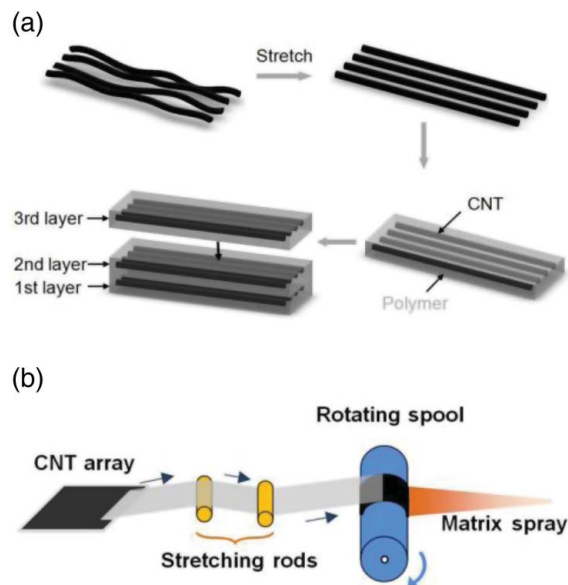


Figure 1. (a) Schematic illustration of the concept of straightening CNTs before embedding them in a polymer matrix in a layer-by-layer fashion. (b) Schematic illustration of the experimental setup for the stretch-winding process.

pair of stationary rods, the increased tension stretches the CNT sheets. The contact angle between the CNT sheet and the stretching rods was controlled at $150\text{--}165^\circ$ (see the Supplementary online material). The CNT sheet was stretched according to a stretch ratio $(L_{rms} - L_0)/L_0$, where L_{rms} and L_0 are the length of the CNT sheet after and before stretching, respectively. The stretched CNT sheet was then wound onto a rotating cylindrical polytetrafluoroethylene spool.

In this one-step synthesis approach, high-performance imide-extended BMI resin (Designer Molecules Inc.) was used as the matrix system. We used a sprayer to deliver $1.0 \text{ g} \cdot \text{L}^{-1}$ BMI/toluene solution in a layer-by-layer fashion as the CNT sheet was wound onto the spool. This step is critical because it allowed individual CNTs to be integrated with the matrix at the molecular level, which should increase the effectiveness of load transfer. The resultant composites had approximately $\sim 50\text{--}55 \text{ wt}\%$ CNT weight fraction.

For a flexible CNT/BMI composite sheet prepared by the stretch-winding approach, its width is determined by the width of the CNT film pulled out from the spinnable array. A high-quality CNT array will allow the pulling out of a CNT film continuously. The fabrication of a strong and electrically conductive CNT/BMI composite sheet opens up opportunities for many real-world applications, such as textiles (Figure 2(a)) and electrical conductors (Figure 2(b)).

Mechanical Performance For real-world applications such as aerospace structures, a stronger and lighter material allows greater degree of flexibility and capacity. As

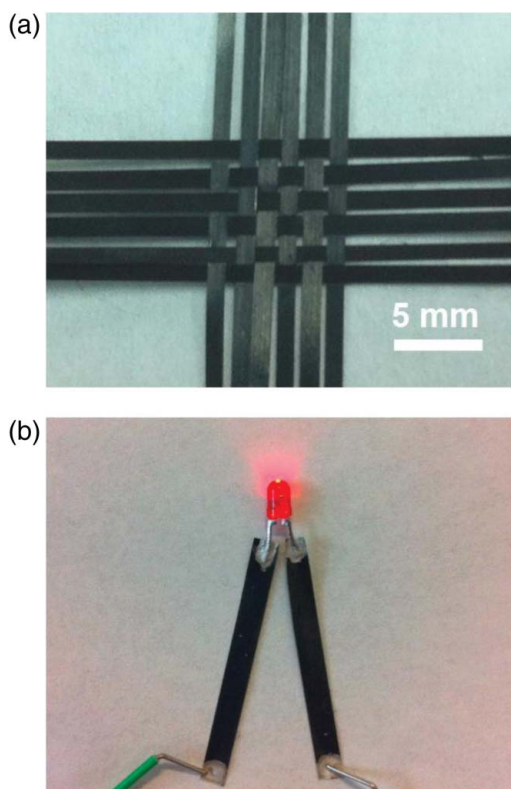


Figure 2. Optical photographs of CNT/BMI composite sheets synthesized by stretch-winding. (a) A textile woven from CNT composite films. (b) The CNT composite films as segments of conductive media loaded with a light-emitting diode (LED) light bulb.

shown in Figure 3(a), our strongest CNT composite is at least 15% stronger than the current best engineering composites, and far higher than those for CNT composites reported previously. In addition, our composites have a lower density of $1.25 \text{ g} \cdot \text{cm}^{-3}$. Consequently, the specific strength of our CNT composites is at least 30% higher than that for the best engineering composites, as shown in Figure 3(b).

The stretch-wound CNT composites have shown an ultrahigh tensile strength of up to 3.8 GPa and a specific strength of up to $3.0 \times 10^7 \text{ cm}$, which represents a significant breakthrough in engineering materials. The average strength and stiffness of four CNT composite samples are 3.5 and 266 GPa, respectively (see the Supplementary online material). Figure 4(a) shows the tensile engineering stress–strain curves of pristine CNT sheet without matrix and CNT composite sheets stretched to various stretch ratios. As shown, the pristine CNT sheet has a strength of 300 MPa and Young's modulus of 21 GPa. The unstretched composites exhibited strength of 2.0 GPa and Young's modulus of 130 GPa. The stretching raised the strength and Young's modulus to as high as 3.8 and 293 GPa, respectively, at the stretch ratio of 12% (Figure 4(b) and (c)). The density of the stretch-wound composites was $1.25 \text{ g} \cdot \text{cm}^{-3}$, as

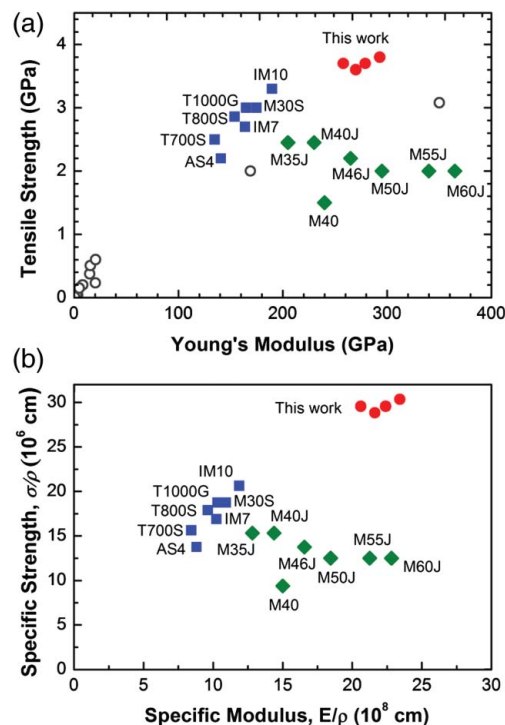


Figure 3. (a) Comparison of the tensile strength and Young's modulus of currently available engineering CFRP as well as CNT composites reported previously. Note that all data are from composite samples. The blue-filled squares are from the existing high-strength CFRP and the green-filled diamonds are from those of the currently existing high-modulus CFRP. The unfilled circles are best CNT composites reported previously [9,22,27]. (b) Comparison of the specific tensile strength and specific modulus of the stretch-wound composites with the best engineering CFRP. These data were calculated based on a density of $1.6 \text{ g} \cdot \text{cm}^{-3}$ for CFRP (60 vol%) and $1.25 \text{ g} \cdot \text{cm}^{-3}$ for the stretch-wound composites (46 vol%).

compared with $1.6 \text{ g} \cdot \text{cm}^{-3}$ for CFRP with a typical 60% fiber by volume. The lower density renders the stretch-wound composites higher specific strength and specific stiffness. The toughness of the stretch-wound composites, calculated as the area under the stress–strain curves, reached $22 \pm 5 \text{ J} \cdot \text{g}^{-1}$, which is higher than that of the recently reported high-strength CNT/BMI composites ($< 15 \text{ J} \cdot \text{g}^{-1}$) [9,27]. The higher toughness ensures safer composite structures with higher damage tolerance.

It should be noted that the stretch winding produced high performance CNT composites without the need for functionalization. The near-perfect structure of nanotubes makes functionalization challenging, as nanotubes are chemically inert and there are hardly any defects to anchor pendant molecules [28]. Functionalization usually creates defects in the nanotube lattice, which compromises their mechanical properties. The stretch-winding approach has successfully overcome the obstacles for conventional methods and bypassed the challenges for CNT functionalization. So far, the strongest non-functionalized CNT composites have a strength of 2 GPa and a stiffness of

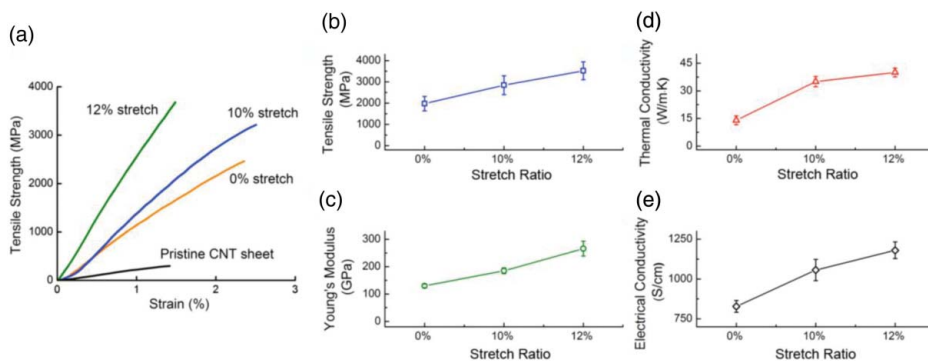


Figure 4. (a) Typical stress–strain curves of pristine CNT sheet, unstretched and stretched composites, demonstrating a significant improvement of the mechanical properties through aligning and straightening of CNTs. Effect of stretching on (b) tensile strength and (c) Young’s modulus, (d) thermal conductivity, and (e) electrical conductivity of the composites.

169 GPa [27], which are much lower than those of our CNT composites.

Thermal and Electrical Properties The room temperature thermal properties of CNT/BMI composites with different stretch ratio are presented in Figure 4(d). The in-plane thermal diffusivities of the composite sheet along the CNT alignment direction, α , were measured using a scanning laser heating analyzer (Ulvac-Riko, Inc., Laser PIT) [29]. The thermal conductivities of the composites, λ , were calculated using $\lambda = \alpha\rho C$, where ρ is the density and C is the specific heat of the composite. The in-plane thermal diffusivity of the 12%-stretched composites averaged $27 \text{ mm}^2 \cdot \text{s}^{-1}$ (see the Supplementary online material), which is three times as high as the value of unstretched composites. For the nanocomposites with 46 vol% CNTs, the calculated λ value is $41 \text{ W m}^{-1} \text{ K}^{-1}$, which is higher than that of unidirectional polyacrylonitrile-based CFRP ($4.5 \text{ W} \cdot \text{m}^{-1} \cdot \text{K}^{-1}$) [30] and other reported high volume fraction CNT composites ($0.4\text{--}1.3 \text{ W} \cdot \text{m}^{-1} \cdot \text{K}^{-1}$) [31]. These results indicate that stretching improves the alignment and straightness of CNTs and promotes a more efficient transfer of phonons along the CNT length direction of the composites.

Composites with straightened CNTs also revealed excellent electrical conductivities because the inter-tube contacts for electron transfer were facilitated by the improved CNT alignment and reduced waviness. The pristine CNT sheets, which were condensed with ethanol, had a highly porous structure and thus a relatively low conductivity of $570 \text{ S} \cdot \text{cm}^{-1}$. The unstretched composites showed an electrical conductivity of $820 \text{ S} \cdot \text{cm}^{-1}$, in which the capillary force of dilute BMI solution drew and held the CNTs close to each other. As shown in Figure 4(e), the electrical conductivity of the composites increases monotonically with increasing stretch ratio. Composite sheets that are stretched for 12% have the highest level of CNT alignment and straightness among all of the samples and thus the highest conductivity of $1230 \text{ S} \cdot \text{cm}^{-1}$, which is a 116% increase over the pristine CNT sheets.

Structural Characteristics After fabricating composite sheets, it is essential to characterize the CNT alignment degree in the polymer nanocomposites, because it significantly affects the mechanical and physical properties. One common approach to statistically characterize CNT alignment is polarized Raman spectroscopy, which is shown in Figure 5(a) and (b) for a composite sheet before and after 12% stretch. Specifically, the shift of the intensity ratio ($I_{G\parallel}/I_{G\perp}$) of G band peaks was measured. Theoretically, Raman intensity change is proportional to $\cos^4 \theta$ versus the CNT orientation angle (θ) [32] at $\theta = 0^\circ$ or when the polarization of the excitation laser’s oscillating electromagnetic field is parallel to the nanotube longitudinal axis, the Raman intensity is maximized because of enhanced absorption, molecular polarization, and optical conductivity [33]. In contrast, at $\theta = 90^\circ$, the Raman scattering from the SWNTs displays a minimum value. Therefore, the ratio of the intensity of the G-band in the parallel configuration to the perpendicular configuration ($I_{G\parallel}/I_{G\perp}$) can be used to describe CNT alignment degree: higher CNT alignment degree should result in a higher intensity ratio. As shown in Figure 5(a), the intensity ratio is approximately 1.6, typical of an unstretched CNT composite sheet. Following the stretch-winding process, the intensity ratio for the 12%-stretched sheet is increased to 7.6, as shown in Figure 5(b), suggesting that the stretch-winding process significantly improves the alignment of CNTs in the nanocomposites. Therefore, the improved CNT alignment is correlated with the observed improvements in mechanical, thermal and electrical properties of the composites.

In addition to the polarized Raman spectroscopy, scanning electron microscopy (SEM) images in Figure 5(c) and (d) also reveal significant improvement in alignment by stretching. To reveal the CNT alignment in the composite, the BMI matrix was removed by heating the composite samples in a thermogravimetric analysis furnace under an inert atmosphere. The unstretched samples showed curved CNTs and large amount of voids although they were aligned macroscopically (Figure 5(c)). In comparison, the stretched composites contained more

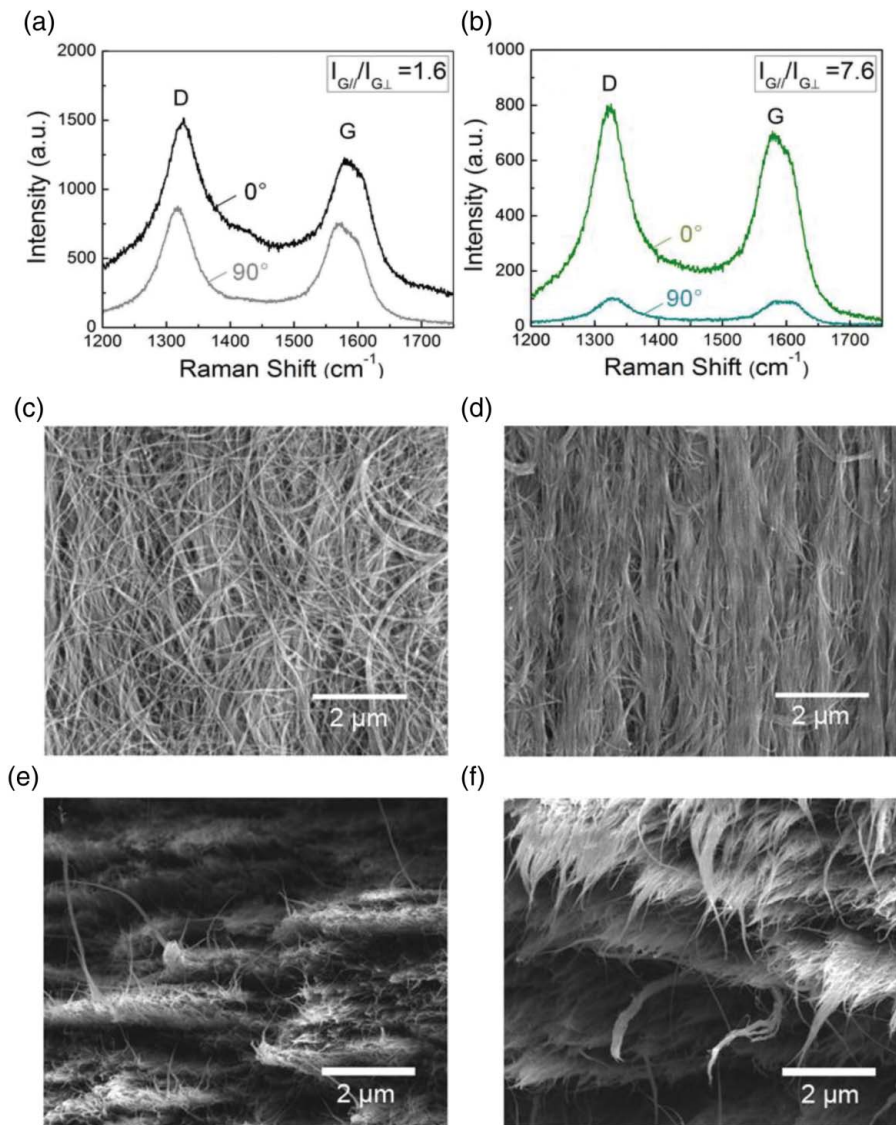


Figure 5. Polarized Raman spectra of the D and G bands from (a) an unstretched composite sheet and (b) a composite sheet stretched by 12%. 0° corresponds to a configuration where the polarization direction of the laser light is parallel to the CNT alignment direction, while 90° corresponds to a configuration where the direction of laser light polarization is perpendicular to the CNT alignment. SEM images of CNT alignment in (c) an unstretched composite sheet with wavy nanotubes and microscale porous structure and (d) a composite sheet stretched by 12%, showing straight, well-aligned and closely-packed nanotubes. SEM images of typical fracture morphologies of (e) an unstretched composite sheet and (f) a composite sheet stretched by 12%.

aligned and straight CNTs (Figure 5(d)), which consequently reduced the voids and improved the contacts between the nanotubes.

Figure 5(e) and (f) shows the morphologies of the fractured surfaces of unstretched and stretched composites, respectively. High volume fraction, good matrix penetration, and a layered failure mode were observed for all of the composites. The layered failure mode is probably due to the spray method since one layer might be already dry before the next one was sprayed on, not allowing for complete polymer migration between layers. Compared with the unstretched sample, the stretched one shows longer CNT pullout length.

In summary, we have shown MWNT/BMI composite sheets with a combination of record-high tensile strength and high stiffness, and excellent thermal and electrical conductivities, which has not been reported in any other engineering composites. These CNT composite sheets were synthesized by a novel technique, stretch-winding, that can incorporate high volume fraction of long CNTs into a polymer matrix while simultaneously aligning and straightening them. In addition, the stretch-winding process can directly make CNT composites or composite prepreps, bypassing the functionalization of CNTs or the slow and expensive step of CNT fiber production. This new approach has the potential

to produce high-performance CNT composite in the industrial scale at low cost, paving the road to their practical structural applications, such as aerospace composite materials, unidirectional thermal interface materials and photovoltaics.

Finally, it is noted that a critical factor for producing high-strength CNT composites is to synthesize high-quality CNT arrays that consist of long and strong individual CNTs and are conducive to pulling-out of continuous and uniform CNT ribbon. However, producing CNT arrays with consistent high-quality has been a challenge for almost all laboratories. This is an issue that needs to be overcome for commercial scale production.

Supplementary online material A more detailed information on experiments is available at <http://dx.doi.org/10.1080/21663831.2012.686586>.

Acknowledgements The work was supported by the North Carolina Space Grant and the Air Force Office of Scientific Research. The measurement of thermal conductivity was performed at the Oak Ridge National Laboratory's High Temperature Materials Laboratory, which was sponsored by the U. S. Department of Energy, Office of Energy Efficiency and Renewable Energy, Vehicle Technologies Program.

References

- [1] Iijima S. Helical microtubules of graphitic carbon. *Nature* 1991;354(6348):56–8.
- [2] Zhang XF, Li QW, Tu Y, Li YA, Coulter JY, Zheng LX, Zhao YH, Jia QX, Peterson DE, Zhu YT. Strong carbon-nanotube fibers spun from long carbon-nanotube arrays. *Small* 2007;3(2):244–8.
- [3] Xie XL, Mai YW, Zhou XP. Dispersion and alignment of carbon nanotubes in polymer matrix: A review. *Materials Science Engineering R* 2005;49(4):89–112.
- [4] Jia ZJ, Wang ZY, Xu CL, Liang J, Wei BQ, Wu DH, Zhu SW. Study on poly(methyl methacrylate)/carbon nanotube composites. *Materials Science Engineering A* 1999;271(1):395–400.
- [5] Moniruzzaman M, Du FM, Romero N, Winey KI. Increased flexural modulus and strength in SWNT/epoxy composites by a new fabrication method. *Polymer* 2006;47(1):293–8.
- [6] Feng QP, Yang JP, Fu SY, Mai YW. Synthesis of carbon nanotube/epoxy composite films with a high nanotube loading by a mixed-curing-agent assisted layer-by-layer method and their electrical conductivity. *Carbon* 2010;48(7):2057–62.
- [7] Wang D, Song PC, Liu CH, Wu W, Fan SS. Highly oriented carbon nanotube papers made of aligned carbon nanotubes. *Nanotechnology* 2008;19(7):075609.
- [8] Bradford PD, Wang X, Zhao H, Maria J-P, Jia Q, Zhu YT. A novel approach to fabricate high volume fraction nanocomposites with long aligned carbon nanotubes. *Composites Science and Technology* 2010;70(13):1980–5.
- [9] Cheng QF, Wang B, Zhang C, Liang ZY. Functionalized carbon-nanotube sheet/bismaleimide nanocomposites: mechanical and electrical performance beyond carbon-fiber composites. *Small* 2010;6(6):763–7.
- [10] Jiang KL, Li QQ, Fan SS. Nanotechnology: Spinning continuous carbon nanotube yarns – Carbon nanotubes weave their way into a range of imaginative macroscopic applications. *Nature* 2002;419(6909):801.
- [11] Li QW, Zhang XF, DePaula RF, Zheng LX, Zhao YH, Stan L, Holesinger TG, Arendt PN, Peterson DE, Zhu YT. Sustained growth of ultralong carbon nanotube arrays for fiber spinning. *Advanced Materials* 2006;18(23):3160–3.
- [12] Liu K, Sun YH, Chen L, Feng C, Feng XF, Jiang KL, Zhao YG, Fan SS. Controlled growth of super-aligned carbon nanotube arrays for spinning continuous unidirectional sheets with tunable physical properties. *Nano letters* 2008;8(2):700–5.
- [13] Jiang KL, Wang JP, Li QQ, Liu LA, Liu CH, Fan SS. Superaligned carbon nanotube arrays, films and yarns: A road to applications. *Advanced Materials* 2011;23(9):1154–61.
- [14] Zhang XF, Li QW, Holesinger TG, Arendt PN, Huang JY, Kirven PD, Clapp TG, DePaula RF, Liao XZ, Zhao YH, Zheng LX, Peterson DE, Zhu YT. Ultrastrong, Stiff, and Lightweight Carbon-Nanotube Fibers. *Advanced Materials* 2007;19(23):4198–201.
- [15] Li QW, Li Y, Zhang XF, Chikkannanavar SB, Zhao YH, Danglewicz AM, Zheng LX, Doorn SK, Jia QX, Peterson DE, Arendt PN, Zhu YT. Structure-dependent electrical properties of carbon nanotube fibers. *Advanced Materials* 2007;19(20):3358–63.
- [16] Zheng LX, Zhang XF, Li QW, Chikkannanavar SB, Li Y, Zhao YH, Liao XZ, Jia QX, Doorn SK, Peterson DE, Zhu YT. Carbon-nanotube cotton for large-scale fibers. *Advanced Materials* 2007;19(18):2567–70.
- [17] Zhang XB, Jiang KL, Teng C, Liu P, Zhang L, Kong J, Zhang TH, Li QQ, Fan SS. Spinning and processing continuous yarns from 4-inch wafer scale super-aligned carbon nanotube arrays. *Advanced Materials* 2006;18(12):1505–10.
- [18] Zhang M, Atkinson KR, Baughman RH. Multifunctional carbon nanotube yarns by downsizing an ancient technology. *Science* 2004;306(5700):1358–61.
- [19] Liu K, Sun YH, Lin XY, Zhou RF, Wang JP, Fan SS, Jiang KL. Scratch-resistant, highly conductive, and high-strength carbon nanotube-based composite yarns. *ACS Nano* 2010;4(10):5827–34.
- [20] Tran CD, Lucas S, Phillips DG, Randeniya LK, Baughman RH, Tran-Cong T. Manufacturing polymer/carbon nanotube composite using a novel direct process. *Nanotechnology* 2011;22(14):145302.
- [21] Fang C, Zhao JN, Jia JJ, Zhang ZG, Zhang XH, Li QW. Enhanced carbon nanotube fibers by polyimide. *Applied Physics Letters* 2010;97(18):181906–181906-3.
- [22] Cheng QF, Wang JP, Wen JJ, Liu CH, Jiang KL, Li QQ, Fan SS. Carbon nanotube/epoxy composites fabricated by resin transfer molding. *Carbon* 2010;48(1):260–6.
- [23] Cheng QF, Wang JP, Jiang KL, Li QQ, Fan SS. Fabrication and properties of aligned multiwalled carbon nanotube-reinforced epoxy composites. *Journal of Materials Research* 2008;23(11):2975–83.
- [24] Liu W, Zhang XH, Xu G, Bradford PD, Wang X, Zhao HB, Zhang YY, Jia QX, Yuan FG, Li QW, Qiu YP, Zhu YT. Producing superior composites by winding carbon nanotubes onto a mandrel under a poly (vinyl alcohol) spray. *Carbon* 2011;49(14):4786–91.
- [25] Wang X, Bradford PD, Liu W, Zhao HB, Inoue Y, Maria JP, Li QW, Yuan FG, Zhu YT. Mechanical and electrical property improvement in CNT/Nylon composites through drawing and stretching. *Composites Science Technology*. 2011;71(14):1677–83.

- [26] Zhang YY, Sheehan CJ, Zhai JY, Zou GF, Luo HM, Xiong J, Zhu YT, Jia QX. Polymer-embedded carbon nanotube ribbons for stretchable conductors. *Advanced Materials* 2010;22(28):3027–31.
- [27] Cheng QF, Bao JW, Park J, Liang ZY, Zhang C, Wang B. High mechanical performance composite conductor: Multi-walled carbon nanotube sheet/bismaleimide nanocomposites. *Advanced Functional Materials* 2009; 19(20):3219–25.
- [28] Ajayan PM, Tour JM. Materials science - Nanotube composites. *Nature* 2007;447(7148):1066–8.
- [29] Veca LM, Meziani MJ, Wang W, Wang X, Lu FS, Zhang PY, Lin Y, Fee R, Connell JW, Sun YP. Carbon nanosheets for polymeric nanocomposites with high thermal conductivity. *Advanced Materials* 2009;21(20):2088–92.
- [30] Pan CT, Hocheng H. Evaluation of anisotropic thermal conductivity for unidirectional FRP in laser machining. *Composites Part A* 2001;32(11):1657–67.
- [31] Yang K, Gu MY, Guo YP, Pan XF, Mu GH. Effects of carbon nanotube functionalization on the mechanical and thermal properties of epoxy composites. *Carbon* 2009;47(7):1723–37.
- [32] Fischer JE, Zhou W, Vavro J, Llaguno MC, Guthy C, Haggenueller R, Casavant MJ, Walters DE, Smalley RE. Magnetically aligned single wall carbon nanotube films: Preferred orientation and anisotropic transport properties. *Journal of Applied Physics* 2003;93(4): 2157–63.
- [33] Ajiki H, Ando T. Aharonov-Bohm effect in carbon nanotubes. *Physica B* 1994;201:349–52.